

Miniaturized Magnetic Nitrogen DC Microplasmas

Chester G. Wilson and Yogesh B. Gianchandani

Abstract—This paper explores the use of miniaturized magnets to enhance the parameters of dc microplasmas. The microplasmas are powered by thin coaxial electrodes and are enhanced by a coaxial magnetron configuration machined from niobium composite magnets. At operating pressures of 1–4 torr, a glow region that is confined to the volume directly over the cathode, forms a traditional magnetron-type annular ring. Three coaxial magnets, ranging in total size from 3.2 to 7.2 mm in outside diameter generate measured magnetic fields up to 3030 G. The magnetic field structure is profiled with a small Hall probe and is modeled by finite-element analysis. The plasma currents for various applied voltages are measured, and the plasma breakdown/termination voltages are determined. In nitrogen ambients at 1.2 torr and 370-V bias, the current changes from 9.3 mA in the absence of a magnetic field to 17.6 mA with the addition of the largest magnet. The sheath region decreases with the addition of the magnetic structures, illustrating an effect on the Debye length and, therefore, the local plasma density. The dimensions of the sheath are found to vary radially within the annular microplasma. The smallest sheath corresponds to the region of highest magnetic field over the south pole for the largest magnetic configuration. This effect is used to generate a microplasma in SF₆ on a silicon wafer producing a localized etch. The etch rate in the region of the brightest glow is three times greater than the weakest etch rate, allowing spatially localized etch selectivity without masking.

Index Terms—Magnetic confinement, manufacturing, microdischarge, microplasma, sensing.

I. INTRODUCTION

MAGNETIC enhancement and confinement of plasmas for manufacturing and sensing offer many opportunities for micromachined devices if the relevant parameters can scale well. Magnetron plasma systems have been widely studied due to their widespread use as sputter-deposition systems. Numerous experimental studies of the dc magnetron have been conducted. The discharge current in magnetrons has been found to increase considerably with a small increase in voltage at 5–10 mtorr pressures, and 100- to 1000-G-type magnetic fields [1]. The gas density in front of the cathode region has been found to be a function of the magnetron current, as a result of neutral heating and gas rarefaction [2]. The resultant effect of the gas densities modification on the voltage-current relation was explored [3]. Optical emission studies have been performed for magnetron discharges in the 5–20-mtorr range [4], [5]. The radial current distributions have been measured and modeled [6], and magnetron plasmas characterized with Langmuir probes [7]. The sheath in magnetrons have been found to vary spa-

tially, with a dependence on the local magnetic field and corresponding current density [1], [8]. A variety of magnetron modeling efforts have been done, including fluid [9], kinetic [10], and Monte-Carlo efforts [11]. All of these efforts describe magnetrons of tens of centimeters in dimension, operating in the millitorr regime, with magnetic field strengths on the order of hundreds of Gauss.

This effort demonstrates magnetically enhanced dc microplasmas. In contrast to conventional (larger scale), on-chip microplasmas and microdischarges are generated by electrodes fabricated on a substrate. These microplasmas and microdischarges have been shown to have potential microsystems applications. These applications include localized silicon etching [12], [13], spectroscopic detection of water impurities, and tunable UV sources [14], [15]. Other applications include gas spectroscopy [16], [17], and display technology [18]. In addition, micro-hollow-cathode discharges have been shown to have several possible applications as radiation sources [19], [20]. All of these potential applications rely on the localization of the microplasmas or microdischarges within a miniaturized, on-chip structure, or on self-confinement of the microdischarge, and require smaller (millimeter to micrometer scale) on-chip electrodes, higher power densities, and higher gas pressures, ranging from 1 torr to atmosphere. However, existing literature is scarce on microplasma devices utilizing miniature magnets to enhance the local parameters. This paper explores magnetic shaping of microdischarges. With a view toward using this technology in microsensors, only miniature magnets are used. The experimental apparatus for this work is described in Section II, followed by experimental results in Section III.

II. EXPERIMENTAL SETUP

This section describes the experimental apparatus and its characterization by modeling and calibration. A schematic of the coaxial magnet assembly that was used is illustrated in Fig. 1, along with the coordinate conventions. Planar electrodes are constructed on a phenolic board with a circular cathode surrounded by a concentric anode. Underneath the cathode is a coaxial magnet structure. The structure has a circular magnet with the north pole facing the electrode, surrounded by a concentric magnet, with the south pole facing the electrode. It is formed by machining niobium powder magnets. As microplasmas are confined at higher pressures, with smaller electrode geometries, the magnetic field strength of these configurations must be increased to the kilogauss regime. The radial distance from the center of the electrode is defined as R . H and Z are parallel axes, with the former being the distance above the magnet and the latter being the distance above the electrode. Since the electrode material is 28- μm -thick aluminum foil, $H = Z + 28 \mu\text{m}$. The outer radius of the inner

Manuscript received June 12, 2003; revised November 13, 2003. This work was supported in part by the National Science Foundation.

The authors are with the Electrical Engineering and Computer Science Department, University of Michigan, Ann Arbor, MI 48109 USA, and also with the Department of Electrical and Computer Engineering, University of Wisconsin, Madison, WI 53706 USA (e-mail: chwilsn@engin.umich.edu).

Digital Object Identifier 10.1109/TPS.2004.824005

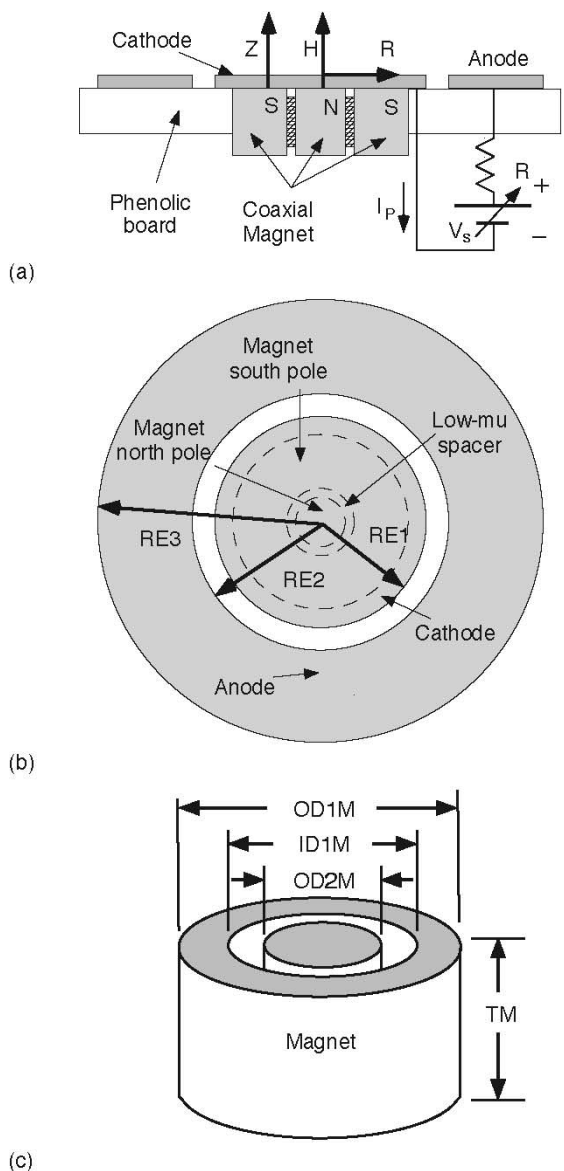


Fig. 1. Schematic illustrating the miniaturized magnetron. (a) Cross section of complete setup showing coordinate system. (b) Top view. (c) Magnet configuration.

TABLE I
TABLE OF COAXIAL MAGNET SIZES

Magnet Size:	Outer diameter 1 OD1M	Inside diameter ID1M	Outside diameter 2 OD2M	Magnet thickness TM
Small	3200	2000	800	4000
Medium	5200	2000	1400	6000
Large	7200	4000	2400	6000

electrode (RE1) is 6.5 mm, the inner and outer radius of the outside electrode, labeled RE2 and RE3, are 7 and 11.5 mm, respectively [Fig. 1(b)]. Three different magnet sizes (large, medium, and small) were used. The magnet and electrode dimensions are illustrated in Fig. 1(c) and cited in Table 1.

Magnetic field equipotential and field line simulations were performed for these magnetic configurations using MAXWELL (Fig. 2). Magnetic equipotential surfaces are shown on the

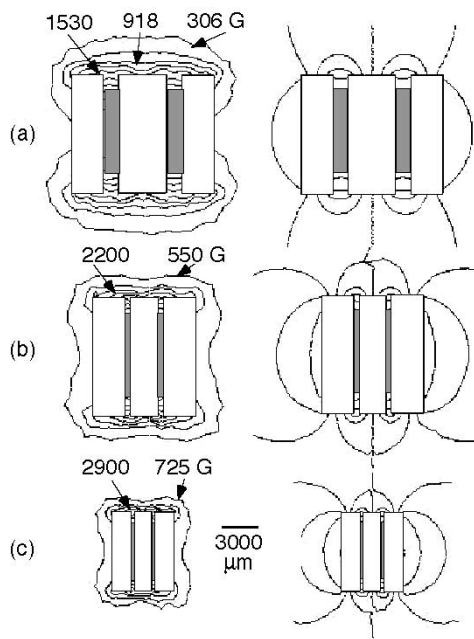


Fig. 2. Simulations of magnetic (left) equipotential surfaces and (right) field lines for (a) large; (b) medium; and (c) small magnet.

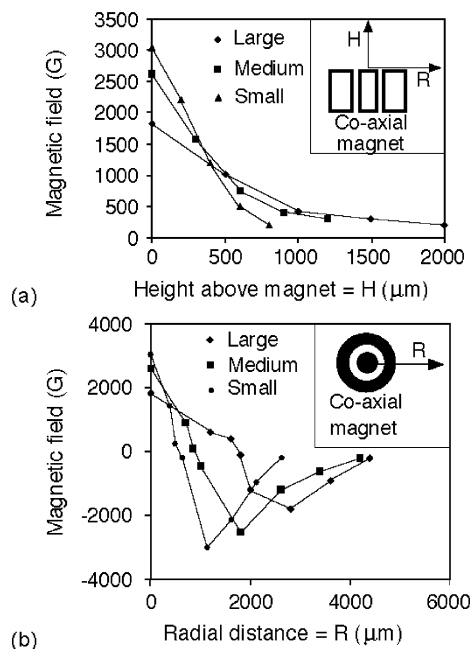


Fig. 3. Measured magnetic field distance H above magnet (a), and in radial direction (b) for coaxial magnets.

left, and field lines on the right. The modeled magnetic field strengths range up to 2900 G, and are larger than typical magnetron field strengths which are typically 500–1000 G. The magnetic field of the coaxial structure was measured using an F.W. Bell BH205 Hall probe, which was chosen for its small sensor footprint. Fig. 3(a) shows the magnetic field in the Z direction, moving upward from the surface of the center of the inside magnet. The magnetic field measured along the radial direction, directly over the surface of the magnet structure is shown in Fig. 3(b). The magnetic field over the north pole is denoted as positive, whereas the field over the south pole is

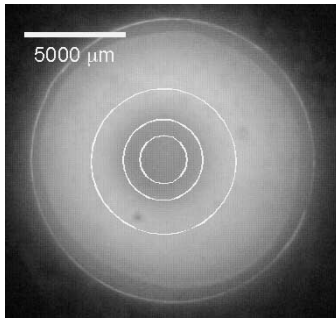


Fig. 4. Local confinement of air microplasma, at 1.2 torr using large magnet. Rings denote magnet profile.

negative. The larger the magnet, the larger the air gap, and the larger the path length of the magnetic field. This results in larger magnetic fields proximate to the surface for smaller magnet configurations. This is seen in both the simulations and measurements with maximum fields at the center of the large, medium, and small magnets measured as 1790, 2410, and 3030 G, and modeled as 1530, 2200, and 2900 G. Measured values are higher than predicted, as the footprint of the probe includes off-center fields, which are higher. As a consequence, the modeled values likely provide greater accuracy for future theoretical and experimental work. Consistent with the magnetic simulations, the measured intensity of the magnetic field extends upwards in the Z direction further for larger magnets. The magnetic field is seen to decay to half strength at 550, 450, and 310 μm above the magnet for the large, medium, and small magnet configurations. The modeled half-strength distances are 705, 494, and 352 μm , respectively. The net result is that the magnetic fields of the larger configurations confine a larger plasma volume, but less well, as the field strength is lower, so the electron gyro-radius is smaller.

III. EXPERIMENTAL RESULTS

A. Plasma Characterization in N_2

The magnet and electrode configurations described in the preceding section were operated in air and N_2 at different pressures ranging from 1.2 to 4 torr. DC power with cathode densities from 0.9 to 5.9 W/cm^2 were used. It was found that all combinations of magnets were effective for confining plasmas within some pressure and power density range. Fig. 4 shows a microplasma generated with the large magnet configuration at 1.2 torr. This section describes the microplasma current driven by the different configurations, breakdown voltages, the internal voltage structure of these microplasmas, and the configurations used in etching silicon.

The magnetic configuration has an impact on both the minimum voltage required to ignite the microplasma and the smaller voltage required to sustain it. In Fig. 5, the right-hand side of a bar corresponds to the voltage at which the microplasma turns on as the voltage is increased, whereas the left hand side is the voltage at which the plasma extinguishes as the voltage is subsequently lowered. At 1.2 torr, the breakdown (ignition) voltage is lowest for the large and medium magnet configurations, while at 4 torr, the breakdown voltage is

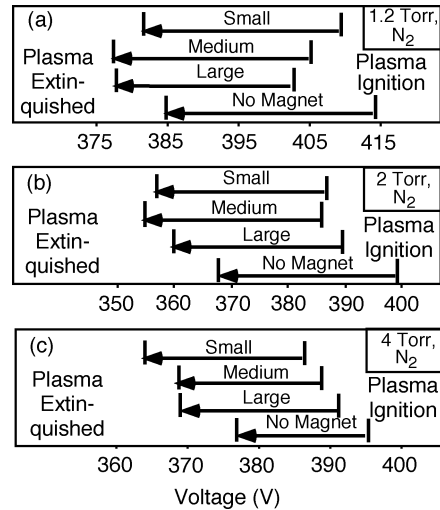


Fig. 5. Plasma ignition and plasma termination with the various magnet sizes for (a) 1.2; (b) 2; and (c) 4 torr.

lowest for the smaller magnet. Magnetic field lines along the breakdown path reduce the plasma initiation voltage. This is expected because the effective path of current is increased by the gyro-radial orbit along the magnetic field lines, resulting in more ionizing collisions. Coplanar electrodes offer a variety of path lengths between the anode and the cathode, as opposed to the constant distance between parallel plates. Microplasmas generated on coplanar electrodes have been found to favor the shorter breakdown paths at higher pressures [13]. The magnetic field lines travel shorter distances in smaller magnets; the magnetic field extends to $R = 2200$ and $R = 4050$ μm for the small and large magnet, respectively [Fig. 3(b)]. This may be the reason that the smallest magnets provide the lowest breakdown voltages at higher pressures.

The current–voltage relationships of magnetically confined microplasmas illustrates a clear trend: the current increases with magnet size. This effect becomes less pronounced at higher pressures. The current–voltage curves for 1.2- and 2-torr operation are shown in Fig. 6. All data was taken for a nitrogen gas ambient. For 1.2 torr, the addition of the large magnet at 370 V increased the plasma current from 9.3 to 17.6 mA, almost doubling it compared to the current in the absence of any magnets [Fig. 6(a)]. However, this fractional increase in current was less at 2 torr [Fig. 6(b)]. These observations are in line with expectations since the fields in the larger magnet configurations occupy more volume.

Traditional scale magnetrons, operating at lower pressures, typically have a particular operational voltage where there is a runaway current, a point of negative differential resistance [1]. This characteristic runaway current was not seen in these microplasmas. This is believed to be due to the relatively high gas pressures that are used. If the electron-neutral mean-free path λ (decreasing with pressure) becomes less than the electron gyro-radius (decreasing with magnetic field strength), confinement is degraded.

Measurements were made of the floating potential of the glow regions, which were located over the cathode. A miniaturized floating potential probe was used to map the floating potential

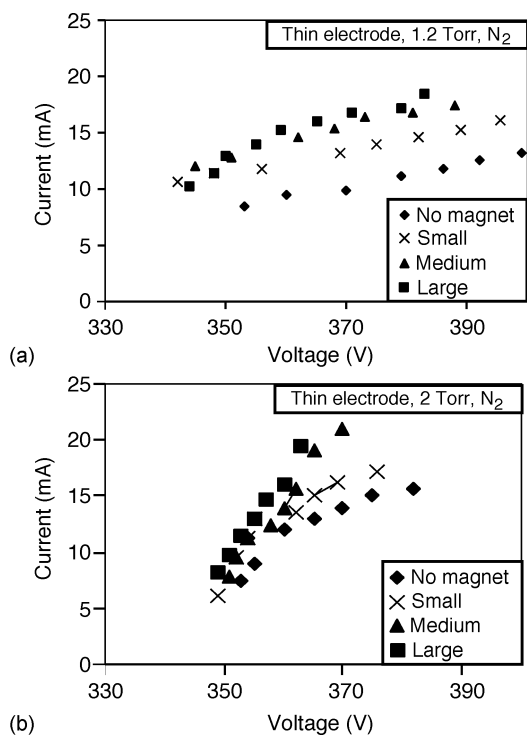


Fig. 6. Measured plasma current as a function of dc voltage at (a) 1.2 and (b) 2 torr.

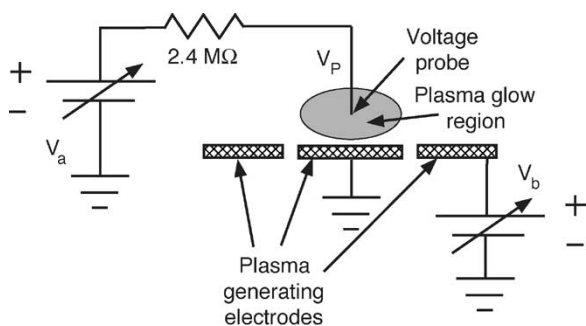


Fig. 7. Circuitry used to measure plasma floating potential.

above the cathode (Fig. 7). The probe, which could be moved radially or along the Z axis was biased with voltage supply V_a through a $2.4\text{-M}\Omega$ resistor. The voltage across the resistor was measured as V_a was increased and when the current through the resistor was zero it was assumed that V_a was the plasma floating potential. The probe was moved vertically down through the glow region (along the Z axis), where the floating potential was found to be fairly uniform. The voltage probe was constructed from a solid copper wire with a diameter of $120\ \mu\text{m}$. The probe was coated with Teflon insulation so that the exposed end formed only a circular metallic cross section. This probe size is small relative to the plasma-generating electrode. In all the measured data shown, the plasma current did not vary by more than 2% throughout even as the probe was moved to map the floating potential; therefore, it can be assumed the probe did not significantly perturb the microplasma.

Floating potential measurements for nitrogen microplasmas taken along the Z axis in the brightest section of the annular

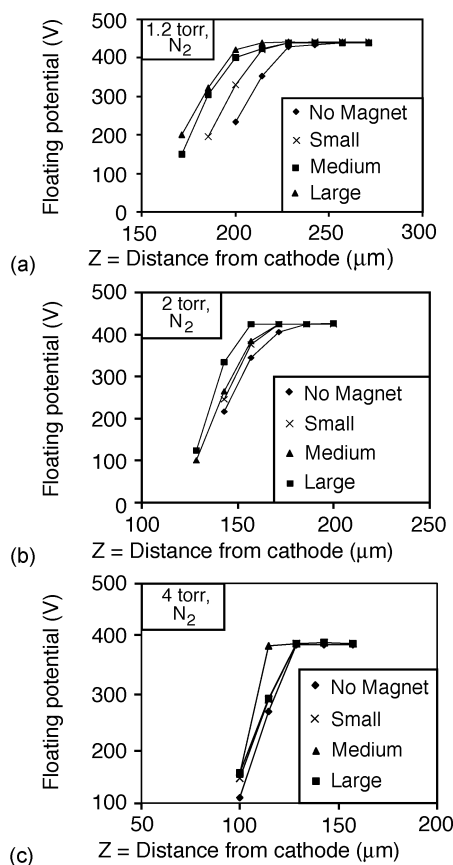


Fig. 8. Floating potential used to measure sheath dimensions: (a) 1.2; (b) 2; and (c) 4 torr.

glow are shown in Fig. 8. The voltage reduces as the probe approaches the sheath region adjoining the cathode. As indicated previously, the height of the sheath decreases in the presence of the magnets and is smallest with the large magnet. The change in the sheath dimensions with the addition of the coaxial magnetic structures is likely due to the localized plasma densities, as the sheath dimension is proportional to the Debye length. This is consistent with the increase in plasma current observed in the presence of magnets. The reduction in sheath height is less pronounced at higher pressures, as electron collisions increase with the reduced mean-free path. Magnetic confinement is reduced when the radial gyro-orbit path becomes greater than the mean free path; electrons cease to be confined along magnetic field lines.

Measurements were made to determine the sheath variation as a function of the radial distance out from the center of the glowing annulus. Fig. 9 shows the case of a nitrogen plasma, at 1.2 torr, with the large magnet. The sheath region is nonuniform, with thinner sheaths corresponding to regions of higher magnetic field. The smallest region of sheath is around $R = 3\text{ mm}$, corresponding to the region of maximum field strength, (-1550 G in the absence of the plasma) over the south pole of the magnet [Fig. 3(b)].

B. Etch Results in SF₆

The large coaxial magnet was utilized in an apparatus similar to that shown in Fig. 1(a), except that a silicon wafer was used as

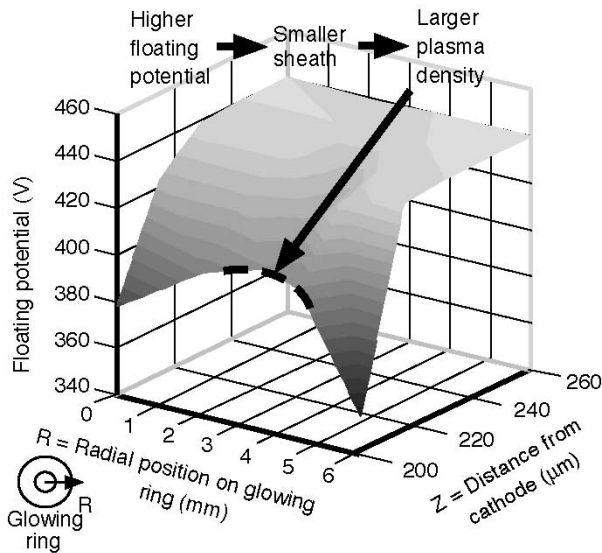


Fig. 9. Floating potential of glow region with large magnet.

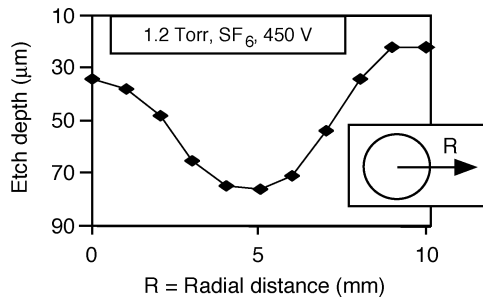


Fig. 10. Etch depth in silicon radially along the ring for a 55-min etch at 1.2 torr with SF₆ gas. Microplasma was operated at 450 V, 0.46 A.

the cathode. The p-type silicon wafer was 170 μm thick and metallized with aluminum on the backside for electrical contact. A plasma ring was generated at 1.2 torr, with an SF₆ ambient gas, using a 450-V power supply, drawing 0.46 A for 55 min. The resulting etch depth varies radially, and corresponds to the dimensions of the glowing ring, with the deepest etching located at the brightest glow regions (Fig. 10). The etch rates for the profile shown in Fig. 10 range from 0.4 to 1.36 μm/s, varying by a factor of three. In contrast, previous work utilizing microplasmas for silicon etching [12] have found that microplasmas generate extremely uniform etch rates at constant power densities, varying only 11% as the feature size is varied from 500 to 6 μm. This demonstrates that microplasmas can be magnetically enhanced at the wafer level for localized silicon etching.

IV. CONCLUSIONS

The properties of microplasmas have been demonstrably modified by magnetic fields generated by permanent magnets ranging from 3.2- to 7.2-mm outside diameter, validating the prospect of a miniature magnetron. Miniaturized magnets were able to generate measured and simulated magnetic field strengths up to 3030 G, required for microplasma enhancement. Current was seen to increase with the addition of the miniaturized magnets, from 9.3 to 17.6 mA for the case of 1.2-torr pressure, and the largest magnet. The magnetic configurations

reduced the sheath dimensions of microplasmas at 1.2 torr, and to a lesser extent at 2 torr. The height of the sheath was nonuniform over the extent of the glow region. It was seen that for the case using largest magnet, the smallest sheath region was in the area of the strongest magnetic field over the south pole. These magnetically enhanced microplasmas were utilized with SF₆ gas to locally etch silicon, resulting in a three-fold difference in etch rates, allowing spatially selective etching without masking. The ability to spatially control microplasma densities and etch characteristics offers promise for use in micromachined manufacturing and sensing applications.

ACKNOWLEDGMENT

The authors would like to thank Prof. A. Wendt for her discussions on magnetron configurations.

REFERENCES

- [1] A. E. Wendt and M. A. Lieberman, "Spatial structure of a planar magnetron discharge," *J. Vac. Sci. Technol. A, Vac. Surf. Films*, vol. 8, no. 2, pp. 902–907, Mar./Apr. 1990.
- [2] S. M. Rossnagel, "Gas density reduction effects in magnetrons," *J. Vac. Sci. Technol. A, Vac. Surf. Films*, vol. 6, no. 1, pp. 19–24, Jan./Feb. 1988.
- [3] S. M. Rossnagel and H. R. Kaufman, "Current-voltage relations in magnetrons," *J. Vac. Sci. Technol. A, Vac. Surf. Films*, vol. 6, no. 2, pp. 19–24, Jan./Feb. 1988.
- [4] L. Gu and M. A. Lieberman, "Axial distribution of optical emission in a planar magnetron discharge," *J. Vac. Sci. Technol. A, Vac. Surf. Films*, vol. 6, no. 5, pp. 2960–2964, Sept./Oct. 1988.
- [5] S. Miyake, N. Shimura, T. Makabe, and A. Itoh, "Diagnosis of direct-current-magnetron discharges by the emission-selected computer-tomography technique," *J. Vac. Sci. Technol. A, Vac. Surf. Films*, vol. 10, no. 4, pp. 1135–1139, July/Aug. 1992.
- [6] A. E. Wendt and M. A. Lieberman, "Radial current distribution at a planar magnetron cathode," *J. Vac. Sci. Technol. A, Vac. Surf. Films*, vol. 6, no. 3, pp. 1827–1831, May/June 1988.
- [7] S. M. Rossnagel and H. R. Kaufman, "Langmuir probe characterization of magnetron operation," *J. Vac. Sci. Technol. A, Vac. Surf. Films*, vol. 4, no. 3, pp. 1822–1825, May/June 1986.
- [8] A. D. Kuypers and H. J. Hopman, "Measurement of ion energy distributions at the powered RF electrode in a variable magnetic field," *J. Appl. Phys.*, vol. 67, no. 3, pp. 1229–1240, Feb. 1990.
- [9] G. Lister, "Influence of electron diffusion on the cathode sheath of a magnetron discharge," *J. Vac. Sci. Technol. A, Vac. Surf. Films*, vol. 14, no. 5, pp. 2736–2743, Sept./Oct. 1996.
- [10] I. A. Porokhova, Y. Golubovskii, J. Bretagne, M. Tichy, and J. F. Behnke, "Kinetic simulation model of magnetron discharges," *Phys. Rev. E, Stat. Phys. Plasmas Fluids Relat. Interdiscip. Top.*, vol. 63, no. 5, pp. 056408/1–056408/9, May 2001.
- [11] S. Kondo and K. Nanbu, "Axisymmetrical particle-in-cell/Monte Carlo simulation of narrow gap planar magnetron plasmas. I. Direct current-driven discharge," *J. Vac. Sci. Technol. A, Vac. Surf. Films*, vol. 19, no. 3, pp. 830–837, June 2001.
- [12] C. Wilson and Y. Gianchandani, "Silicon micro-machining using in-situ dc microplasmas," *IEEE J. Microelectromech. Syst.*, vol. 10, pp. 50–54, Mar. 2001.
- [13] C. G. Wilson, "Microplasmas and microdischarges for manufacturing and sensing applications," Ph.D. dissertation, Univ. Wisconsin, Madison, WI, 2003.
- [14] C. G. Wilson and Y. B. Gianchandani, "LED-SPEC: Spectroscopic detection of water contaminants using glow discharge from liquid electrodes," *IEEE Trans. Electron Devices*, vol. 49, pp. 2317–2322, Dec. 2002.
- [15] G. Jenkins and A. Manz, "Optical emission detection of liquid analytes using a micro-machined dc glow discharge device at atmospheric pressure," *Proc. Micro. Total Anal. Syst.*, pp. 349–350, 2001.
- [16] J. C. T. Eijkel, H. Stoeri, and A. Manz, "A dc microplasma on a chip employed as an optical emission detector for gas chromatography," *Anal. Chem.*, vol. 72, pp. 2547–2552, June 2000.
- [17] J. A. Hopwood, "A microfabricated inductively coupled plasma generator," *J. Microelectromech. Syst.*, vol. 9, no. 3, pp. 309–313, Sept. 2000.

- [18] S. J. Park, J. Chen, C. Liu, and J. G. Eden, "Silicon microdischarge devices having inverted pyramidal cathodes: Fabrication and performance of arrays," *Appl. Phys. Lett.*, vol. 4, no. 78, pp. 419–421, Jan. 2001.
- [19] M. Moselhy, S. Wenhui, R. H. Stark, and K. H. Schoenbach, "A flat glow discharge excimer radiation source," *IEEE Trans. Plasma Sci.*, vol. 30, pp. 198–199, Feb. 2002.
- [20] A. A. Mohamed, R. Block, and K. H. Schoenbach, "Direct current glow discharges in atmospheric air," *IEEE Trans. Plasma Sci.*, vol. 30, pp. 182–183, Feb. 2002.



Chester G. Wilson received the B.S. degree in electrical engineering and the M.S. degree in applied physics from the University of Washington, Seattle, in 1993 and 1996, respectively. He is currently working toward the Ph.D. degree in electrical engineering (in the field of MEMS) at the University of Wisconsin, Madison.

His research interests include plasmas and microfabrication and he is currently studying techniques to scale down silicon-etching plasmas into microplasmas, for practical use in silicon etching,

and to study their physical properties.

Mr. Wilson received the 2000–2001 Intel Foundation Graduate Fellowship Award.



Yogesh B. Gianchandani received the B.S., M.S., and Ph.D. degrees, in electrical engineering in 1984, 1986, and 1994, respectively.

He was with Xerox Corporation, from 1985 to 1988, and with Microchip Technology, from 1988 to 1989, where he worked in the area of integrated circuit design. From 1994 to August 1997, he was a Research Fellow with the Center for Integrated Sensors and Circuits, University of Michigan, Ann Arbor. Since then, he has been an Assistant Professor with the Department of Electrical and Computer Engineering, University of Wisconsin, Madison. He has authored more than 50 published papers in technical conference proceedings and journals and has several patents pending. His research interests include all aspects of design, fabrication, and packaging of micromachined sensors and actuators and their interface circuits.

Prof. Gianchandani received the National Science Foundation Career Award in 2000. He has served as a Section Editor for the journal *Sensors and Actuators* since September 2000, and on the steering committee for the IEEE International Conference on Microelectromechanical Systems (MEMS) since 1999.